2022

A Numerical Modelling Study on Submerged Condensers for Heat Pump Water Heaters Using Low-GWP Refrigerants

Mingkan Zhang

Bo Shen

A Numerical Modelling Study on Submerged Condensers for Heat Pump Water Heaters Using Low-GWP Refrigerants

Mingkan Zhang[1], Bo Shen[1]*

[1]Buildings and Transportation Science Division, Oak Ridge National Laboratory, Oak Ridge, TN 37830, USA

* Corresponding Author: shenb@ornl.gov

ABSTRACT

Challenges to global warming require reduction of GHG emissions, and increased use of renewable energy. Heat pumps extract energy from renewable sources and convert them to more useable forms for space conditioning, space heating and for water heating. They can be powered by renewable sources of electricity and must be engineered to use low global warming potentials (GWP) refrigerants (e.g., propane, GWP = 3) for a sustainable economy. Therefore, an electric heat pump water heaters (HPWH) using propane as refrigerant are developed in Oak Ridge National Laboratory to replace water heaters using all electric resistance and natural gas. A submerged condenser directly contacting with water is employed in the HPWH, which eliminates heat transfer barrier of the tank wall, and also prevents heat loss from the condenser tubes to the surrounding air. In present work, a numerical model is developed to model the submerged condenser. A dynamic temperature distribution on the condenser tubes from experimental data is applied to the model to enhance the accuracy of the numerical model. The model is essential to guide the design of the submerged condenser to achieve the performance required by the HPWH.

1. INTRODUCTION

According to the DOE Buildings Energy Databook (U.S. Department of Energy, 2012), water heating consumed 12.3% total energy in the residential sector of U.S. in 2011, which makes water heating the second largest energy end use for residences. In 2010, the natural gas water heater and electric water heater consumed 1.73 quadrillion Btu and 1.67 quadrillion Btu energy, respectively. Different to conventional gas and electric resistance water heaters, the heat pump water heater is an energy-efficient appliance, which saves up to 70% energy comparing to electric resistance water heaters. Using heat pump heating technologies, HPWHs absorb heat from ambient or indoor air with an evaporator and compress the refrigerant to high pressure and temperature using a compressor. Two types of condensers are usually employed in HPWHs: a) forced water flow heat exchangers like tube-in-tube and brazed plate heat exchangers coupled with a water circulation pump; and b) a water heating coil either wrapped-around the water tank or submerged inside the water tank (no water pump required). Since the submerged condensers can not only eliminate heat transfer barrier of the tank wall, but also prevent heat loss from the condenser tubes to the surrounding air, more and more studies have dedicated on it (Ji *et al.*, 2003; Guo *et al.*, 2011).

Due to the restrictions imposed by the Kyoto Protocol (United Nations, 1998), the current high GWP refrigerants used in heat pumps will be phased down. One of the high GWP refrigerants is R-134a (GWP = 1301), which is the most used refrigerant in HPWHs. Therefore, some studies have been conducted to replace R-134a by other low GWP refrigerants. Gürel et al. (Gürel *et al.*, 2020) assessed four alternative low GWP refrigerants to replace R-134a, including R-290 (GWP = 3), R-600a (GWP = 4), R-1234yf (GWP < 1), and R-1234ze (GWP < 1), to replace R-134a. As the conclusion, the authors recommended R-600a and R-1234ze as the two best candidates to replace R-134a in the refrigeration application. On the other hand, de Paula et al. (de Paula *et al.*, 2020) conducted optimal design and environmental, energy and exergy analysis for R-290, R-1234yf and R-744 (GWP = 1) to replace R-134a. In terms of Total Equivalent Warming Impact and exergy efficiency, their study indicated that R-290 was identified as the optimum option. Another study reported by Duarte (Duarte, 2018) compared the performance of a heat pump water

heater assisted by solar using different refrigerants of R-134a, R-1234yf, R-290, R-744, R-600a. Although at a low solar radiation density, R-134a had the best performance, R-290 showed the best performance at a high and medium solar radiation density. Due to the previous studies, R-290 is a promising low GWP refrigerant to replace R-134a in HPWHs. Therefore, an electric HPWH using R-290 as refrigerant are developed in Oak Ridge National Laboratory to replace water heaters using all electric resistance and natural gas.

In order to assistant the design of the HPWH using low GWP refrigerants, a computational fluid dynamics (CFD) model has been developed to model the HPWH. Building up with the dynamic temperature distribution on the condenser tubes from experimental testing, a simplification approached is employed in the CFD model to avoid complicated multi-phase simulations. The model is capable of providing the insight of the HPWH, including the water temperature distributions, water flow patterns, as well as the temperature history in a specific location in the HPWH. The CFD model provides an economic tool to guide the design of the submerged condenser to achieve the performance required by the HPWH.

2. SIMULATION DOMAIN

A 3D CFD model has been developed using a commercial code Ansys Fluent (Version 17.2) (ANSYS, 2017), which is installed in a workstation with an Intel Xeon E5-2630 v3 processor and 64 GB memory. Figure 1 shows the simulation domain. Working as a condenser, the coils tubes are sandwiched by two pieces of copper sheets. Total twelve tubes are bundled parallelly between the sheets. Then the copper sheets are bended together with the tubes inside. The inner and outer diameters of the bended sheets are 0.150 m and 0.156 m, respectively. The angle between two ends of the cooper sheets after bending is 315°, which leaves a 45° gap in the tank. The bended sheets are filled with thermal paste to enhance the heat transfer between the coils and sheets. Since the diameter of the coils is very small (about 6 mm) comparing the simulation domain size, it is very difficult to directly model the coils in the CFD model. To simplify the model, it is assumed that the bundled 12 coil tubes have the same heat transfer coefficient along their coil lengths. The bundled coil tubes can be simplified to pieces of annuli deployed in the water tank from top to bottom, while the thermal paste occupies the rest space between the sheets. In Figure 1, the yellow annuli are coil tube bundles, and the rest are the thermal paste. In present work, the coil tube bundles, thermal paste, and the two copper sheets called condenser. Then the condenser is merged to a water tank with diameter 0.54 m and heigh 1.25 m, as shown in Figure 1. Therefore, the simulation domain is comprised of a water tank filled with water, coil tube bundles, and thermal paste sandwiched by two copper sheets. It is assumed that the copper sheets are perfectly sealed, and no water can enter the space between the sheets. As a result, in the simulation, water only appears in the tank. The 45° gap provides a path to connect the water inside and outside of the heat exchanger to benefits the heat transfer in the tank. Two types of tube deployments have been modeled in present work. Figure 2 shows the schematic view of the deployments. In Figure 2, the left one represents the evenly deployed tubes bundles with thickness 0.036 m, called even deployment. On the other hand, the right one depicts the mixing phase tubes are centralized to the bottom of the heat exchanger as bottom deployment. The gaps between two adjacent tube bundles are 0.103 m and 0.005 m from the even deployment and bottom deployment, respectively.

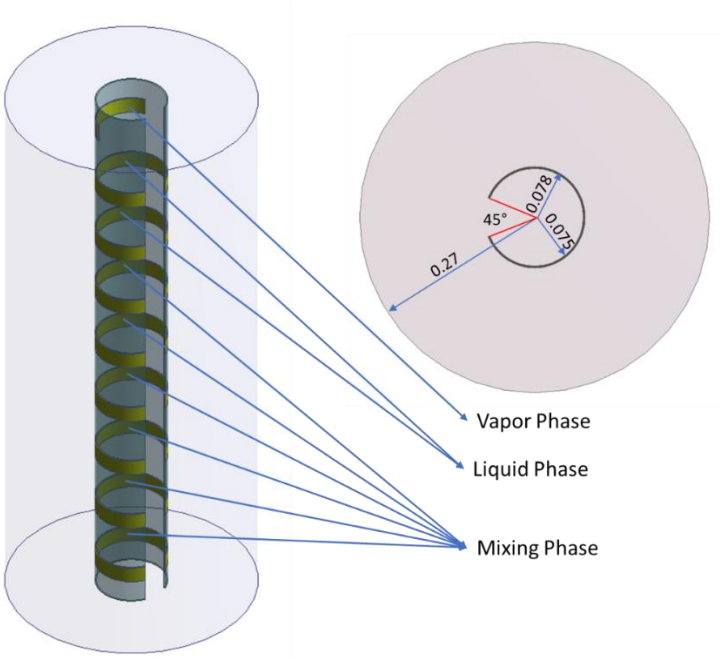

Figure 1 The schematic view of the simulation domain.

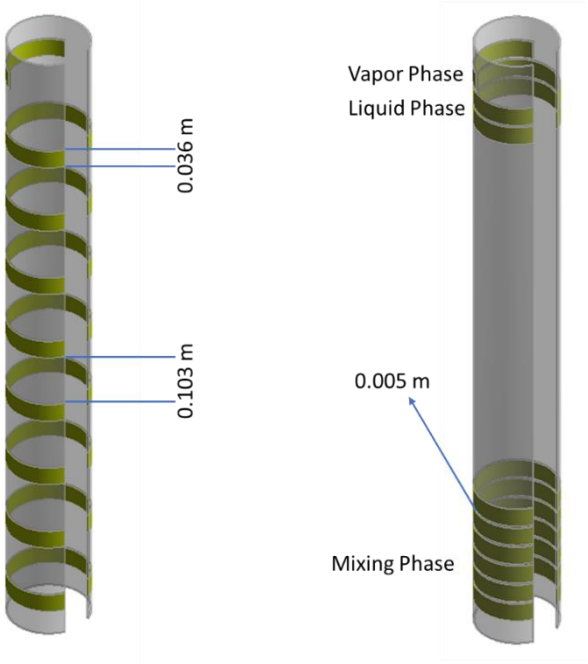

Figure 2 The schematic view of the deployments of submerged condensers

3. MATHEMATICAL MODELS

The governing equations consider for the fluid flow and heat transfer include the continuity, momentum, and energy equations. In the present model, only water flow due to natural convection in the tank is modeled, so in the model, the continuity and momentum equations are written as

$$\frac{\partial \rho}{\partial t} + \nabla \cdot (\rho \boldsymbol{u}) = 0\,, \tag{1}$$

$$\frac{\partial (\rho \boldsymbol{u})}{\partial t} + \nabla \cdot (\rho \boldsymbol{u}\boldsymbol{u}) = -\nabla p + \nabla \cdot \mu \left(\nabla \boldsymbol{u} + \nabla \boldsymbol{u}^{\mathrm{T}} - \frac{2}{3} \nabla \cdot \boldsymbol{u}\boldsymbol{I} \right) + \rho \boldsymbol{g}, \tag{2}$$

where $\boldsymbol{u}$, ρ, p, μ, $\boldsymbol{g}$, and $\boldsymbol{I}$ are fluid velocity vector, density, pressure, dynamic viscosity, gravitational acceleration, and unit tensor, respectively. Therefore, $\rho \boldsymbol{g}$ represents the gravitational body force, which is described by a Boussinesq approximation in present model.

Because the fluid flow is driven by the natural convection, the Reynolds number is low in the water tank. As a result, the water flow is always laminar flow.

The energy equation is

$$\frac{\partial}{\partial t}(\rho E) + \nabla \cdot (\boldsymbol{u}(\rho E + p)) = \nabla \cdot (\lambda \nabla T), \tag{3}$$

where

$$E = h - \frac{p}{\rho} + \frac{|\boldsymbol{u}|^2}{2}. \tag{4}$$

where λ is the thermal conductivity of water. In Eq. (3) and (4), T and h represent the temperature and the enthalpy of water, which are related with Eq. (4).

$$h = \int_{T_{ref}}^{T} c_p \mathrm{d}T + \frac{p}{\rho}\,. \tag{5}$$

where T_{ref} = 298.15 K and c_{p} is the specific heat of water.

When the refrigerant passes the HPWH, it changes phase. Initially, when the refrigerant enters the heat exchanger, with vapor phase. After moving forward in the heat exchanger and heating the water, the refrigerant temperature drops. When it reaches the condensation point, the refrigerant starts condensing, leading to a mixing vapor-liquid phase of refrigerant in the heat exchanger. When it finishes condensing, all the refrigerant turns to liquid phase so only liquid phase of refrigerant can be found in the end of heat exchanger. The coil tubes of the heat exchanger can be divided into three groups according to the refrigerant phase inside, vapor phase, mixing phase and liquid phase. Previous experiments observed that, in each circuit, the beginning 5% length is vapor, the end 23% length is liquid, the middle 72% length contains two-phase refrigerant. Therefore, in the CFD model, the deployment of the coil tubes is shown in Figure 1. Since in the experimental testing, the liquid phase occurs in the tubes retuning to the top of the tank, the liquid phase tubes are deployed between vapor phase and mixing phase tubes.

To avoid complicated condensing simulations, a simplified approach based on experimental observations has been employed in present work. The observations are:

(1) The average mixing temperature is 11°C higher than the average water temperature adjacent to the mixing tubes.

(2) In the mixing region, the temperature drops 5.5°C due to the pressure drop, distributed linearly along the two-phase tube length.

(3) In the vapor section, the temperature drops 5.5°C from entering vapor to the first point of two-phase, distributed linearly along the vapor tube length.

(4) In the liquid section, the temperature drops 11°C, distributed linearly along the liquid tube length.

Building up with the observations from the testing, the simplified approach contains the following steps:

(1) In every time step of the simulation, read the average water temperature adjacent to the mixing tubes, then calculate the average mixing saturation temperature according to the observation (1).

(2) Based on the average mixing saturation temperature and the observation (2), one can calculate the temperature distribution along the mixing tube length.

(3) Since the temperature of the higher end at the mixing tubes equals to the lower end temperature at the vapor tubes, the temperature distribution along the vapor tube length can be caculated by considering observation (3).

(4) Similar to the vapor tubes, the temperature distribution along the liquid tube length can be obtained using the higher end temperature at the liquid tubes and observation (4).

A computer code has been developed to work with FLUENT to control the tubes temperatures in the model as boundary conditions in every time step of the simulation.

Because the geometry is symmetric, only half of the domain is modeled to save the computational time. The initial water temperature in the tank is set as 14.45°C. ANSYS/FLUENT is used to generate the mesh and solve the mathematic models for the heat transfer between the heat exchanger and the water and water flow driven by the natural convection in the tank.

4. RESULTS AND DISCUSSION

The CFD model has been implemented to the two cases, the even and the bottom case, which are shown in Figure 2. In the simulations, the tank is heated for 15 hours with starting temperature 14.45°C for both the cases. Figure 3 shows the velocity vectors in the symmetric face of the water tank for both cases after 15 hours heating. The figure shows the circulating flows due to the natural convection induced by the temperature/density differences. In the even case, due to the even distribution of the tubes, lots of the local circulating flows are generated along the vertical length of the water tank. On the other hand, for the bottom case, because most of the tubes are near the tank bottom, the circulating flows mainly happen near the tank bottom. The local circulating flows are seldomly observed in the bottom case. Instead, a huge circulating flow occurs, which is circled in the figure, due to the temperature difference between top and bottom of the tank.

The different flow patterns from the two cases result in different water temperature distribution in the tank. Figure 4 shows the tank temperature distributions in the symmetric face of the water tank for both cases after 15 hours heating. Due to the natural convection, the temperature stratification can be observed from both cases. The local high temperature region around the tubes can be clearly identified in contours. Note that the two contours use two legends. In the even case, the temperature span in the tank is 12 °C from top to bottom. In the bottom case, the difference is only about 3°C. It is because the tubes are near the bottom of the tank leading to a heating concentration near the tank bottom. In addition, the huge circulating flow benefits the overall heat circulating in the tank. As a result, the temperature span in the bottom case is small. On the other hand, the tubes are evenly distributed in the even case, leading to small local circulating flows. Therefore, the overall heat circulating is weak to end up with a high temperature span in the even case.

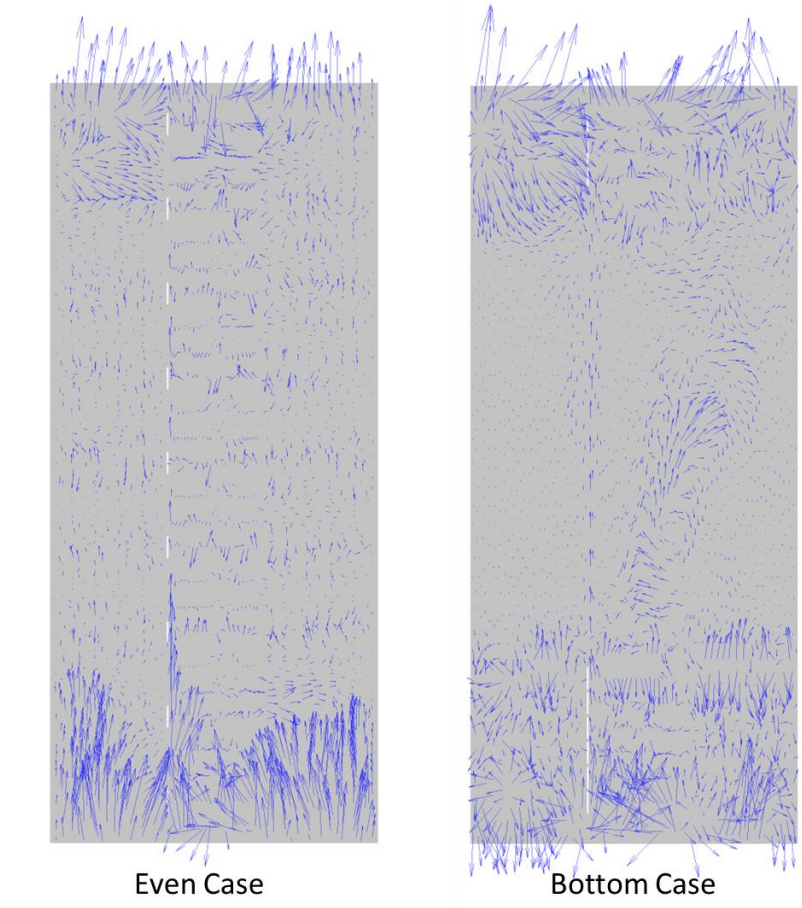

Figure 3 Flow velocity vectors in the tank.

Figure 5 plots the average temperature of the tank (T_{tank}) changing with time, which reveals that in the 15 hours heating, the tank temperature in the even case is always higher than the bottom case, although the difference is small. Therefore, the average tank temperature in the even case with a high temperature span and bottom case with a low temperature span are very close.

Figure 6 plots the temperature at the top of the tank (T_{top}) changing with time, which indicates that the temperature of the tank top keeps increasing in the 15 hours due to the heating. The T_{top} of the even case is always higher than the bottom case. After 15 hours, the T_{top} of the even case is about 60°C, while the bottom case is about 55°C. Therefore, after 15 hours heating, the top temperature of the even case is 5°C higher than the bottom case. It can be found in Figure 4 that in the symmetric face, the top temperature of the bottom case is much lower than the even case.

Building up with the experimental observations, a simplified CFD model has been developed to model submerged condensers. Two different deployments of the tubes simulated. The simulation results shows that the evenly distributed tubes can provide a slightly higher tank temperature than the bottom case. Moreover, the evenly distributed tubes can make the tank top temperature much higher than the bottom case.

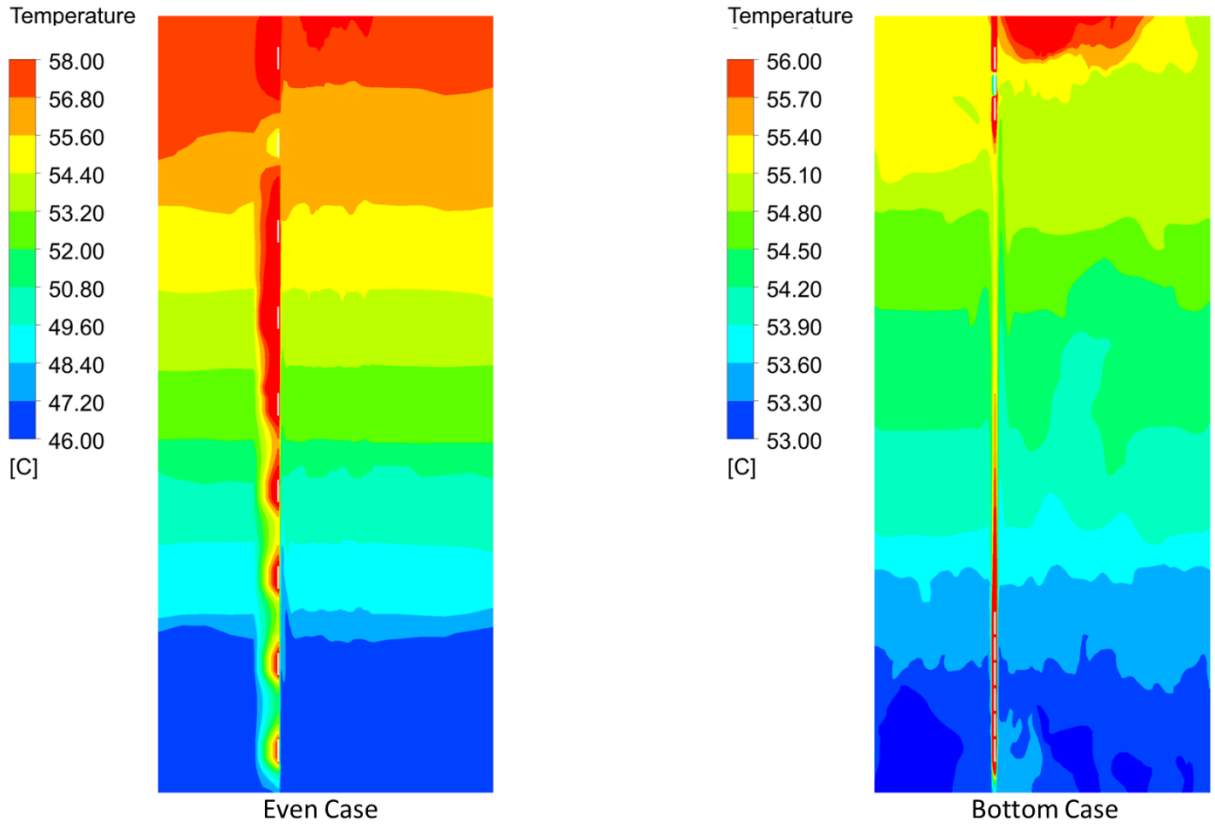

Figure 4 Temperature distributions in tank

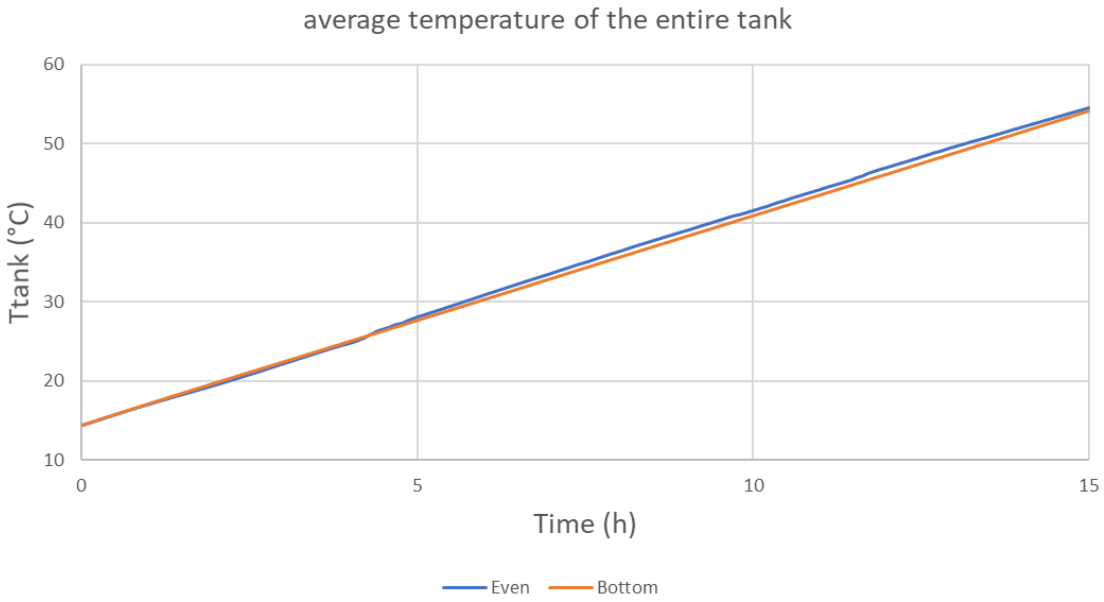

Figure 5 T_{tank} changes with time

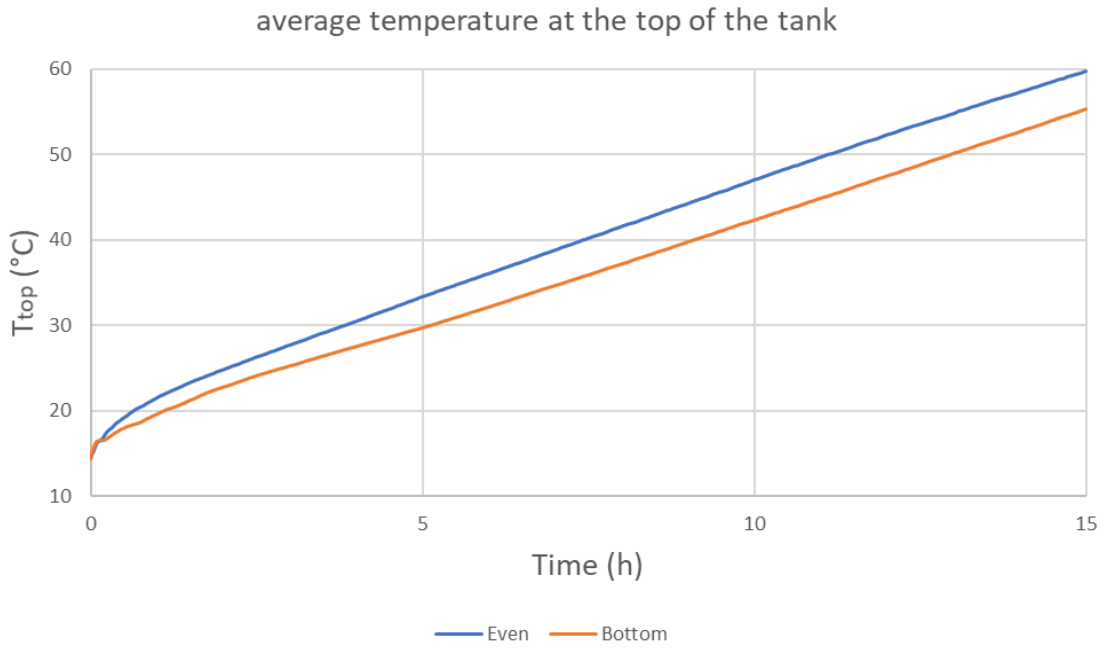

Figure 6 T_{top} changes with time

5. CONCLUSIONS

A CFD model has been developed to model an electric HPWH using R-290 as refrigerant. The model is comprised of a water tank filled with water, coil tube bundles, and thermal paste sandwiched by two copper sheets. Instead of directly modeling the multi-phase flow and heat transfer in the condensers, a simplified approach is used based on observations from experiments to save computational resources. The simulation results provide an insight of the temperature distribution and flow patterns in the HPWH. Two condenser deployments, even case and bottom case,

are tested using the CFD model. The results reveal that although the temperature distribution in the HPWHs with two deployments are different, the average temperatures of the HPWHs are very close. However, due to the temperature distribution difference, the top temperature of the even case is 5°C higher than the bottom case.

REFERENCES

ANSYS (2017) *ANSYS FLUENT 17.2 Theory Guide*.
Duarte, W. M. (2018) *Numeric model of a direct expansion solar assisted heat pump water heater operating with low gwp refrigerants (R1234yf, R600a and R744) for replacement of R134a*. Available at: https://repositorio.ufmg.br/handle/1843/BUOS-B8UHX4 (Accessed: 5 April 2022).
Guo, J. J. *et al.* (2011) 'Experimental research and operation optimization of an air-source heat pump water heater', *Applied Energy*, 88(11), pp. 4128–4138. doi: 10.1016/j.apenergy.2011.04.012.
Gürel, A. E. *et al.* (2020) 'Energy, exergy, and environmental (3e) assessments of various refrigerants in the refrigeration systems with internal heat exchanger', *Heat Transfer Research*, 51(11), pp. 1029–1041. doi: 10.1615/HEATTRANSRES.2020033716.
Ji, J. *et al.* (2003) 'Domestic air-conditioner and integrated water heater for subtropical climate', *Applied Thermal Engineering*, 23(5), pp. 581–592. doi: 10.1016/S1359-4311(02)00228-4.
de Paula, C. H. *et al.* (2020) 'Optimal design and environmental, energy and exergy analysis of a vapor compression refrigeration system using R290, R1234yf, and R744 as alternatives to replace R134a', *International Journal of Refrigeration*. Elsevier Ltd, 113, pp. 10–20. doi: 10.1016/j.ijrefrig.2020.01.012.
U.S. Department of Energy (2012) *2011 Buildings Energy Data Book, Office of Energy Efficiency and Renewable Energy*. Available at: http://buildingsdatabook.eren.doe.gov/ChapterIntro2.aspx%5Cnhttp://buildingsdatabook.eren.doe.gov/docs/DataBooks/2011_BEDB.pdf.
United Nations (1998) *Kyoto protocol to the united nations framwork convention on climate change.* Kyoto, Japan.

ACKNOWLEDGEMENT

This work was sponsored by the U. S. Department of Energy's Building Technologies Office under Contract No. DE-AC05-00OR22725 with UT-Battelle, LLC. We would like to acknowledge Dr. Isaac Mahderekal the Technology Manager for the HVAC & Appliances for his support.